Thermal Science and Engineering Progress 55 (2024) 102927

Contents lists available at ScienceDirect

Thermal Science and Engineering Progress

journal homepage: www.sciencedirect.com/journal/thermal-science-and-engineering-progress

Multi-objective optimisation of hybrid renewable energy systems for Colombian non-interconnected zones

José Luis Torres-Madroñero [a], César Nieto-Londoño [a,b,*], Erika Arenas-Castiblanco [a], Zulamita Zapata-Benabithe [a], Hussam Jouhara [c,d]

[a] Grupo de Energía y Termodinámica, Escuela de Ingenierías, Universidad Pontificia Bolivariana, Medellín 050031, Colombia
[b] Grupo de Investigación en Ingniería Aeroespacial, Escuela de Ingenierías, Universidad Pontificia Bolivariana, Medellín 050031, Colombia
[c] Heat Pipe and Thermal Management Research Group, College of Engineering, Design and Physical Sciences, Brunel University London, UB8 3PH, UK
[d] Vytautas Magnus University, Studentu Str. 11, LT-53362 Akademija, Kaunas Distr., Lithuania

ARTICLE INFO

Keywords:
Particle swarm optimisation
Hybrid renewable energy systems
Noninterconected Zones

ABSTRACT

Colombia's Atlantic coast wind and solar resources could enhance energy mix and self-generation. Renewable clean energy has been studied in response to fossil fuel pollution. Wind and solar photovoltaic systems have low initial, operational, and levelized energy costs. Variable wind and sun radiation may limit availability. In this regard, hybrid renewable energy systems (HRES) and energy storage have become crucial. These systems can effectively meet load demand by utilising complementary renewable resources. This study deals with sizing a wind and photovoltaic HRES with storage, using a Particle Swarm Optimisation algorithm for yearly variable resources in a non-interconnected zone in La Guajira, Colombia. The study evaluates the *LCOE*, probability of load loss, and the system's CO_2 emission. It develops a sensitivity analysis to determine the importance of each objective factor. From a life cycle analysis, an HRES configuration with low *LCOE* and environmental emission rates is associated with the size of the wind resource; the HRES configuration with minimum *LCOE* values is close to obtaining higher equivalent CO2e emissions. The study highlights the configuration obtained for the Colombian context, giving more importance to the environmental factor and reaching an *LCOE* of 0.754 USD/kWh and emission of 18.97 tCO_2e/year; this configuration also increases the wind energy generation, reaching 41 % more share, compared to the configuration obtained when the economic factor is a priority.

1. Introduction

The energy sector is essential in developing countries [1,2]. Fossil fuels provide 66 % of the world's energy demand and are responsible for global warming and environmental pollution. Additionally, with the increase in the world population, around 1.2 billion people worldwide cannot access electricity [3,4]. In these circumstances, renewable energies have been presented as a solution to the planet's increasing temperature and environmental pollution, as well as to supply the constantly growing energy demand and the scarcity of fossil resources [5,6].

Renewable energies depend on stochastic natural resources in a specific location [3], presenting a mismatch between electricity generation and the energy demand of the region [1,7]. This way, more than one renewable energy source will be needed to meet the energy demand [8]. Hybrid Renewable Energy Systems (HRES) stand out due to their capability to integrate two or more renewable energy sources. In this regard, wind and solar photovoltaic generation have become the most implemented HRES combination due to their complementarity [5]. These systems can also include backups, such as battery banks, to supply energy when the dynamics of renewable sources are insufficient [7,9]. Additionally, HRES can improve off-grid systems' power supply reliability [10]. It makes them less dependent on conventional fossil fuel-based generation and reduces environmental pollution. Nevertheless, with the advantages mentioned above of HRES, these systems require optimisation of their size and operation to obtain those benefits at the lowest cost [7]. Artificial Intelligence optimisation methodologies such as Particle Swarm Optimisation (PSO) have been used to size these systems [8]. PSO is mainly based on the migratory movements of fish and birds [11], and their advantage is the highest exploration capability in each iteration [12], related to their simple implementation, high precision, and convergence [13].

Most of the works on HRES sizing optimisation use economic criteria

* Corresponding author at: Grupo de Energía y Termodinámica, Escuela de Ingenierías, Universidad Pontificia Bolivariana, Medellín 050031, Colombia.
E-mail address: cesar.nieto@upb.edu.co (C. Nieto-Londoño).

https://doi.org/10.1016/j.tsep.2024.102927
Received 30 April 2024; Received in revised form 28 August 2024; Accepted 21 September 2024
Available online 23 September 2024

Nomenclature

a	Life of the hybrid system
c_1	Learning factors for $x_{best,\,p}$
c_2	Learning factors for $x_{g,\,best}$
CO_2e	CO_2 equivalent emission
CRF	Capital recovery factor
$C_{capital}$	Initial capital cost
$C_{c,b}$	Capital cost of the storage system
$C_{c,inv}$	Capital cost of converter
$C_{c,wt}$	Wind turbine's initial cost
$C_{c,pv}$	Photovoltaic solar panel's initial cost
C_{mtto}	Maintenance-operation cost
$C_{m,wt}$	Maintenance cost of the wind turbine system
$C_{m,pv}$	Maintenance cost of the photovoltaic system
DOD	Maximum discharge percentage
E_{ca}	Energy demand
E_b	Battery energy state
$E_{b,min}$	Minimum state of battery charge
E_{ren}	Total renewable energy generation by HRES
E_{pv}	Total photovoltaic generation
E_{wt}	Total wind power generation
ER_{CO_2}	CO_2e emission rate
ER_{wt,CO_2}	CO_2e emission rate of wind generation
$ER_{pv,\,CO_2}$	CO_2e emission rate of photovoltaic generation
ER_{B,CO_2}	CO_2e emission rate of battery storage system
$f_{obj,CO2}$	Normalised expression for the CO_2 emission rate
$f_{obj,E}$	Normalised evaluation of the economic factor
$f_{obj,T}$	Normalised evaluation of the technical factor
GHG	Greenhouse Gases
HRES	Hybrid Renewable Energy System
ir	Interest rate
it	Iteration in PSO optimisation
LCA	Life cycle assessment
$LCOE$	Levelized Cost of Energy
$LPSP$	Loss of Power Supply Probability
$LC_{CO_2,wt}$	Specific GHG emissions by wind generation
$LC_{CO_2,pv}$	Specific GHG emissions by photovoltaic generation
$LC_{CO_2,B}$	Specific GHG emissions by battery storage system
M	Multi-objective function
n_{ch}	Characteristics of particles (PSO)
$NOCT$	Operating temperature of the solar cell
N_b	Number of batteries
N_{inv}	Number of converters
N_{pv}	Number of photovoltaic panels
N_{wt}	Number of wind turbines
N_T	Temperature coefficient of photovoltaic panel
PSO	Particle Swarm Optimisation
p_{PSO}	Particles generated by PSO
P_{pv}	Photovoltaic power generation
P_{pvr}	Nominal power of the photovoltaic panel
P_r	Nominal power of the wind turbine
P_{wt}	Wind power generation
r_1, r_2	Random values (PSO)
r_b	Charge or discharge rate in operation of battery
r_{rb}	Maximum charge and discharge rate of battery
R	Solar radiation
R_{ref}	Reference solar radiation
S_b	Battery nominal capacity
t	Time
TAC	Total annual cost
T_{ref}	Reference temperature of the solar cell
T	Ambient temperature
v	Wind speed.
v_p	Velocity of each particle (PSO)
$v_{p,pso}$	Current velocity of each particle (PSO)
V_{ci}	Cut-In wind speed
V_{co}	Cut-Off wind speed
V_r	Nominal wind speed
w_{CO2}	Weight of the environmental evaluation
w_{pso}	Learning factor corresponding to the velocity (PSO)
w_E	Weight of the economic factor
w_T	Weight of the technical factor
WSA	Weight sensitivity analysis
x_p	Position of each particle (PSO)
$x_{best,\,p}$	Best position of each particle (PSO)
$x_{g,\,best}$	Position of the best particle (PSO)
σ	Self-discharge ratio of the battery
η_{bat}	Efficiency of the battery
η_{inv}	Efficiency of the converter

as the objective function, such as minimising the cost of energy, and technical criteria, such as minimising the *LPSP* (probability of loss of power supply) [11,14,15]. However, other criteria have recently been involved in optimisation functions seeking to consider sustainability aspects, such as job creation and environmental issues. Rakibul Hassan et al. [16] modelled an HRES using a non-dominated sorting genetic algorithm II (NSGA-II) considering three objective functions: Cost of Energy (CoE), Job Creation (JC) and Lifecycle Emission (LCE). They applied a fuzzy decision-making method to select the best trade-off solution. On the other hand, Mojan Maleki et al. [17] optimised the size of an HRES, including economic, environmental, energy security, and technical factors. These authors used HOMER to obtain some of the best HRES configurations based on financial criteria, then applied the TOPSIS method (Technique for Order Preference by Similarity to the Ideal Solution) for multi-criteria decision-making that involves environmental, energy security and technical aspects to determine the optimal HRES. Weights for each element in the objective function are assigned using two methods: AHP (Analytical Hierarchy Process) and weights based on the number of sustainable development goals (SDG 1–7) related to each aspect.

The weights of each factor within the multi-objective functions are input parameters that can affect the search and sizing of the best solution [18]. If the economic factor is the most determinant, the optimisation algorithm can obtain systems with oversized power generation, higher pollution rates, or low diversity in the generation sources. Similarly, the parameterisation with equal weights for all factors tends to reduce the accuracy of the optimisation method in the search for a solution [19]. For its part, sensitivity analysis is a versatile tool that allows you to examine and understand the results of a change in the input parameters. In this way, critical values that impact the results can be revealed, and more reliable models and results can be obtained [20].

The purpose of this work is to size a hybrid energy system composed of wind and photovoltaic solar generation, in addition to a battery bank system, using a PSO optimisation methodology, to supply the energy demand of an area isolated from the electrical grid in Colombia, specifically a rural area in the department of La Guajira. Economic, technical, and environmental aspects are the main components of the objective function. The model evaluates variable wind and solar resources throughout a year of operation and allows the calculation of the loss of power supply probability (*LPSP*), levelized cost of energy (*LCOE*), and the CO_2e emission rate. A weighting method by sensitivity analysis was developed to determine the effect of each factor on the optimal configuration. All formulations regarding the comprehensive evaluation of the HRES are presented in Sections 2.1 to 2.3. Section 2.4 presents the PSO calculation iteration process. Section 3 shows the reference conditions for study cases. Finally, Section 4 develops the result analysis and discussion, and Section 5 summarises the main conclusions reached.

2. Materials and methods

This section presents the models for assessing the energy, economic and environmental behaviour of the HRES evaluated using a Particle Swarm Optimisation (PSO) approach. The mathematical models were integrated into the Python environment for several study cases, considering wind, solar and battery bank technologies, among other factors.

2.1. Energy formulation

This subsection shows the mathematical formulation for generating, using, and storing electricity for a hybrid system using a mix of wind turbines, photovoltaic panels, and batteries. In this regard, wind power generation for a horizontal wind turbine as a function of time t is evaluated as follows:

$$P_{wt}(t) = \begin{cases} 0 & v(t) < V_{ci} \\ \dfrac{P_r}{(V_r^3 - V_{ci}^3)}v^3(t) - \dfrac{V_{ci}^3}{(V_r^3 - V_{ci}^3)}P_r & V_{ci} \le v(t) < V_r \\ P_r & V_r \le v(t) < V_{co} \\ 0 & v(t) \ge V_{co} \end{cases} \tag{1}$$

with V_{ci}, V_r, V_{co} the Cut-In, nominal and Cut-Off speed, respectively. P_r is the nominal power of the wind turbine, and $v(t)$ is the wind speed at time t [21]. In this sense, the total wind generation $E_{wt}(t)$ is equal to the product of $P_{wt}(t)$ and the number of wind turbines N_{wt}. Since this study does not consider a factor of the area occupied by the hybrid generation system, the required separation between turbines to avoid mutual interference in wind generation was not considered.

On the other hand, the power generation of a photovoltaic system is given by:

$$P_{pv}(t) = P_{pvr}\frac{R(t)}{R_{ref}}\left[1 + N_T(T_c(t) - T_{ref})\right] \tag{2}$$

with $T_c(t) = T(t) + \left[\left(\frac{NOCT-20}{800}\right)R(t)\right]$, with P_{pvr} the nominal power of the panel, $R(t)$ the solar radiation, R_{ref} the reference solar radiation, T_{ref} the reference temperature of the solar cell, N_T the temperature coefficient of the panel, $T(t)$ the ambient temperature, and $NOCT$ the operating temperature of the solar cell [22]. Therefore, the total photovoltaic generation $E_{pv}(t)$ is the product of $P_{pv}(t)$ and the number of panels N_{pv}.

The battery state depends on the comparison between the demand and the electricity generation as follows:

$$E_b(t) = \begin{cases} E_b(t-1)(1-\sigma) + \left\{\left[\left(E_{pv}(t)\eta_{inv} + E_{wt}(t)\eta_{inv}^2\right) - \dfrac{E_{ca}(t)}{\eta_{inv}}\right]\eta_{bat}\right\} & E_{pv}(t) + E_{wt}(t) > E_{ca}(t) \\ E_b(t-1)(1-\sigma) - \left\{\dfrac{\left[\dfrac{E_{ca}(t)}{\eta_{inv}} - \left(E_{pv}(t)\eta_{inv} + E_{wt}(t)\eta_{inv}^2\right)\right]}{\eta_{bat}}\right\} & E_{pv}(t) + E_{wt}(t) < E_{ca}(t) \end{cases} \tag{3}$$

where $E_b(t-1)$ is the previous state of the battery, σ is the self-discharge ratio of the battery, η_{inv} is the efficiency of the converter, η_{bat} is the efficiency of the battery and $E_{ca}(t)$ is the energy demand [23]. The batteries have a maximum charge and discharge rate r_{rb}, given in percentage fraction by the manufacturer, and the charge or discharge rate in operation r_b, as follows [24]:

$$r_b = \frac{|E_b(t-1) - E_b(t)|}{E_b(t-1)} \tag{4}$$

where $r_b \in [0,1]$. This way, restrictions are defined for the charging and discharging of the storage system. Additionally, another restriction for batteries is the minimum state of charge as a function of the maximum discharge percentage, DOD, and its nominal capacity, S_b, given as [22]:

$$E_{b,min} = (1 - DOD)S_b. \tag{5}$$

The total renewable energy $E_{ren}(t)$ takes into account the total generation of renewable energy (i.e., $E_{gen}(t) = N_{wt}P_{wt}(t) + N_{pv}P_{pv}(t)$), the storage system contribution, and the energy stored. In this way, if the generation by the renewable devices (i.e., wind turbines and/or photovoltaic panels), exceeds the demand, the system will charge the battery system. Meanwhile, if the energy generated does not supply the energy demand, the storage system must provide additional energy to the demand. On the other hand, if the renewable system at same time generates energy equal to the demand, the battery system stores energy until its maximum storage capacity [25]. Finally, when the renewable electricity generation or the battery supply cannot meet the demand, the technical factor of loss of supply probability will measure the amount of missing electrical energy. In this sense, the comparison between the total renewable energy generation $E_{ren}(t)$ and the demand $E_{ca}(t)$ gives the Loss of Power Supply Probability, $LPSP$, over the total hours of a year, given as:

$$LPSP = \frac{\sum_{t=1}^{8760}[E_{ca}(t) - E_{ren}(t)]}{\sum_{t=1}^{8760}E_{ca}(t)} \tag{6}$$

Considering the above formulation, if the load required exceeds the electricity generation by the HRES, the $LPSP$ value will be greater than zero; on the other hand, if the electricity generation exceeds the demand, the $LPSP$ value is less than zero. In this sense, negative $LPSP$ values mean that the electricity generated by the HRES system is oversized to demand. Moreover, the evaluation of $LPSP$ will have a maximum value $LPSP_{max}$ at an instant of time, a positive value means that, for at least one instant, the demand is not satisfied by the renewable energy system generation, and a negative value implies that the electricity generation of the HRES meets the load demand [23].

2.2. Economic formulation

The Levelized Cost of Energy, $LCOE$, is calculated for the economic evaluation. It determines the monetary value for each kWh generated, and it is given by [26]:

$$LCOE = \frac{TAC}{\sum_{t=1}^{8760} E_{ren}(t)} \tag{7}$$

where TAC is the total annual cost equal to the sum of the initial capital cost, $C_{capital}$, and maintenance-operation costs, C_{mtto}, expressed as follows:

$$C_{capital} = CRF(N_{wt}C_{c,wt} + N_{pv}C_{c,pv} + N_bC_{c,b} + N_{inv}C_{c,inv}) withCRF = \frac{ir(1+ir)^a}{(1+ir)^a - 1} \tag{8}$$

$$C_{mtto} = N_{wt}C_{m,wt} + N_{pv}C_{m,pv} \tag{9}$$

where $C_{c,wt}$ is the wind turbine's initial cost, $C_{c,pv}$ is the photovoltaic solar panel's initial cost, N_b is the quantity of batteries, N_{inv} is the number of converters, $C_{c,b}$ and $C_{c,inv}$ are the capital cost of the storage system and converter with a lifetime of five years and ten years, respectively; $C_{m,wt}$ and $C_{m,pv}$ are the maintenance cost of the wind turbine and the photovoltaic solar panel, respectively. Additionally, CRF, is the Capital Recovery Factor defined as a function of interest rate, ir, and the life of the hybrid system, a (i.e., 20 years) [25].

2.3. Environmental evaluation

One of the most used methodologies for the environmental evaluation of an electricity generation project is the life cycle assessment (LCA) [27–29], in which the adverse effects on the environment can be quantified from the measurement of Greenhouse Gases (GHG) emissions based on the mass of equivalent CO_2 emitted for each kWh generated (gCO_2e/kWh) [30]. The LCA methodology integrates three stages of an electric energy project. The first stage, called Upstream, corresponds to the extraction of resources, manufacturing materials and components, and construction of the electrical energy generation system. The second stage, or Operation, is related to the operation and maintenance of the generation system. The third stage, Downstream, is the final disposal after the system reaches the end of its useful life [30].

For each stage, the literature provides approximate GHG values for each form of electricity generation. In the operation stage, the new forms of renewable energy stand out compared to traditional forms of generation [31], such as gas or coal, obtaining lower GHG emissions values. Coal-based electricity generation reaches 1,000 gCO_2e/kWh, while renewable generation only achieves emissions of between 10 gCO_2e/kWh and 40 gCO_2e/kWh, values corresponding to wind and photovoltaic generation, respectively [27,30]. However, in the Upstream stage, forms of generation using fossil fuels obtain lower GHG values than renewable energies. Solar photovoltaic and wind power generation are of particular interest to this study. For photovoltaic energy, the emissions levels throughout its life cycle are attributed 60 % to the Upstream stage, 20 % to Operation and another 20 % to the Downstream stage [32]. The CO_2e emissions from wind generation correspond to 86 % of the exploitation and manufacturing stage, 9 % of the operation, and 5 % of the final disposal of the system [33]. The above values can be compared with electricity generation from coal, where less than 1 % is Upstream, more than 98 % is in operation, and less than 1 % is at final disposal [32,33].

Table 1
Estimation of CO_2e emission rate.

Renewable Electric Generation	GHG emission Equation	Specific GHG emissions [gCO2e/kWh]
Wind Turbine	$ER_{wt,CO_2} = LC_{CO_2,wt}E_{wt}$	$LC_{CO_2,wt} = 13$
Solar Photovoltaic	$ER_{pv,CO_2} = LC_{CO_2,pv}E_{pv}$	$LC_{CO_2,pv} = 43$
Battery Storage Supply	$ER_{B,CO_2} = LC_{CO_2,B}E_{BS}$	$LC_{CO_2,B} = 33$

Following the above discussion, the CO_2e emissions rate can be calculated knowing the total electricity generation for each renewable energy generation over one year of operation as summarized in Table 1. The specific CO_2e emissions $LC_{CO_2,wt}$ for wind generation, $LC_{CO_2,pv}$ for photovoltaic generation, and $LC_{CO_2,B}$ battery deliver energy, were fixed as 13 gCO_2e/kWh, 43 gCO_2e/kWh and 33 gCO_2e/kWh, respectively [30,32,33]. For this study, emissions for wind and solar photovoltaic generation considering the electricity delivered from the battery bank are evaluated as follows:

$$ER_{CO_2} = LC_{CO_2,wt}E_{wt} + LC_{CO_2,pv}E_{pv} + LC_{CO_2,B}E_{BS} \tag{10}$$

where $LC_{CO_2,wt}$ and $LC_{CO_2,pv}$ are the specific GHG emissions measured in gCO_2e/kWh for wind and solar photovoltaic generation, respectively; E_{wt} and E_{pv} are calculated using Equations (1) and (2), respectively. Equation (10) also includes the emission rate due to the use of the battery bank by a hybrid system as the product between $LC_{CO_2,B}$ and E_{BS}, corresponding to the CO_2e emissions and the electricity delivered by battery storage; in this sense, the factor $LC_{CO_2,B}$ is given only when the storage system delivers electricity to the hybrid system [30].

2.4. PSO formulation

The Particle Swarm Optimisation (PSO) is presented in the flowchart of Fig. 1. The optimization process begins with the creation of p_{PSO} particles with n_{ch} characteristics; the last corresponds to the total combination of wind turbines, solar panels, and batteries. Each particle is evaluated with a multi-objective search according to the following equation:

$$M = w_Tf_{obj,T} + w_Ef_{obj,E} + w_{CO2}f_{obj,CO2} \tag{11}$$

where w_T is the weighting of the technical factor $f_{obj,T}$, w_E is the weighting of the economic factor $f_{obj,E}$, w_{CO2} is the weighting of the environmental evaluation by $f_{obj,CO2}$, where the sum of them must be equal to one.

In this sense, the normalised evaluation of the technical factor ($LPSP$) is $f_{obj,T}$, the normalised evaluation of the economic factor ($LCOE$) is $f_{obj,E}$, and $f_{obj,CO2}$ is the normalised expression for the CO_2 emission rate, all of them for each particle [34]. The normalisation for the $LPSP$ is set with a reference value of 4 %, which is an approximate value of the energy losses in the Colombian rural sector [35], for the $LCOE$ the normalisation is with the sum of the reference values of 0.038 USD/kWh, 0.036 USD/kWh, and 0.125 USD/kWh for the wind energy, photovoltaic energy and battery storage system, respectively [36]. The normalised value for the CO_2e emission rate is 50,000 $kgCO_2$/year, an average value obtained for different forms of electric generation reported by Mandal et al. [27], who studied the optimum sizing of an HRES for a rural zone with a load demand of 243 kWh/day. The hybrid system comprised solar photovoltaic, wind, and diesel-electric generation. Table 2 reviews the above normalisation methodology.

The best position of each particle and the best position among all particles are identified. The restriction in the reliability of the HRES is calculated for $LPSP$ values less than the reference value defined above; if this criterion is not reached or the iteration number is the maximum, the algorithm ends, and the best particle is selected. Meanwhile, the algorithm continues with the calculation of the velocity of each particle given by:

$$v_p(it+1) = w_{pso}\,v_{p,pso}(it) + c_1\,r_1\left(x_{best,\,p}(it) - x_p(it)\right) + c_2\,r_2\left(x_{g,\,best}(it) - x_p(it)\right) \tag{12}$$

where $x_p(it)$ is the position of each particle in the iteration it, $x_{best,p}(it)$ is the best position of each particle, $x_{g,best}(it)$ is the position of the best particle, $v_{p,pso}(it)$ is the velocity of each particle, w_{pso} is the learning

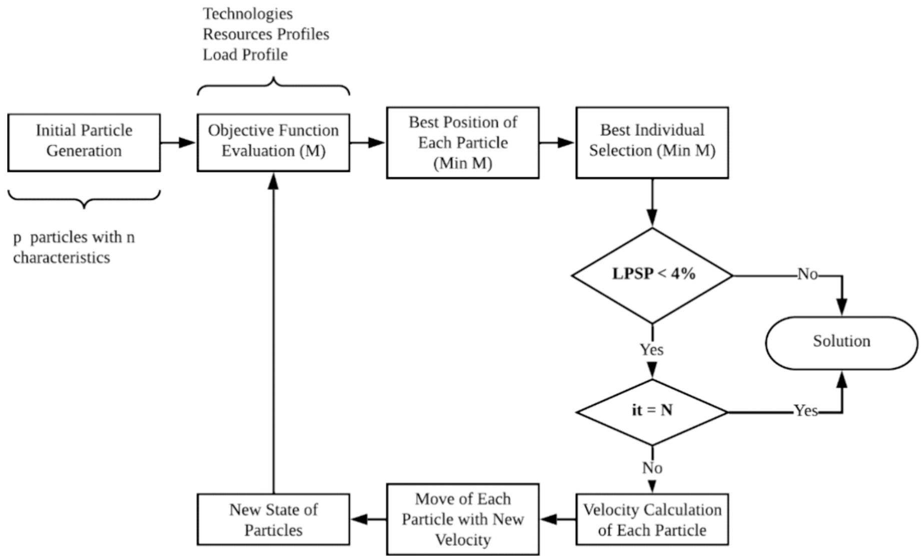

Fig. 1. PSO optimisation flowchart [25].

Table 2
Normalisation Methodology.

Type of Factor	Factor	Normalised expression	Reference Normalised Value
Technical	Loss Power Supply Probability, *LPSP*	$f_{obj,T}$	4 %
Economic	Levelized Cost of Energy,*LCOE*	$f_{obj,E}$	0.038 USD/kWh + 0.036 USD/kWh + 0.125 USD/kWh
Environmental	CO_2e emissions rate,ER_{CO_2}	$f_{obj,CO2}$	50,000 kgCO_2/year

factor corresponding to the velocity at iteration it, c_1 and, c_2 are the learning factors, r_1 and r_2 are random values, obtaining independence between the particle evaluation. For the above $v_p(it+1)$ is the new velocity that determines the new position of each particle as a function of the current particle position $x_p(it)$, according to [25] and [37]:

$$x_p(it+1) = v_p(it+1) + x_p(it) \tag{13}$$

3. Reference conditions and PSO assessment parameters

The PSO methodology developed for sizing HRES is initially assessed considering wind speed and solar radiation resources over one year every hour (8,760 h). The reference wind resources are plotted in Fig. 2 as wind speed frequency. These reference cases are a profile that follows a distribution between 0 m/s and 12 m/s, which is a typical safety range operation of commercial small wind turbines, where a right bias (Case A), a standard (Case B) and a left bias (Case C) distribution are considered. A case with the typical wind speed resource from Puerto Bolivar, La Guajira, Colombia, is named Case D in the sizing process [38].

The aim of evaluating wind probability distributions with different statistical trends is to determine the effect of the wind resource on the selection of the best solution obtained by applying the optimisation method with the technical, economic and environmental factors. In this way, the wind speed required to start the generation by the wind turbine is decisive; as highlighted below, the cut-in speed of the small wind turbine considered in this study is 2 m/s. In this sense, the wind resource with the right bias distribution will have its highest probability of

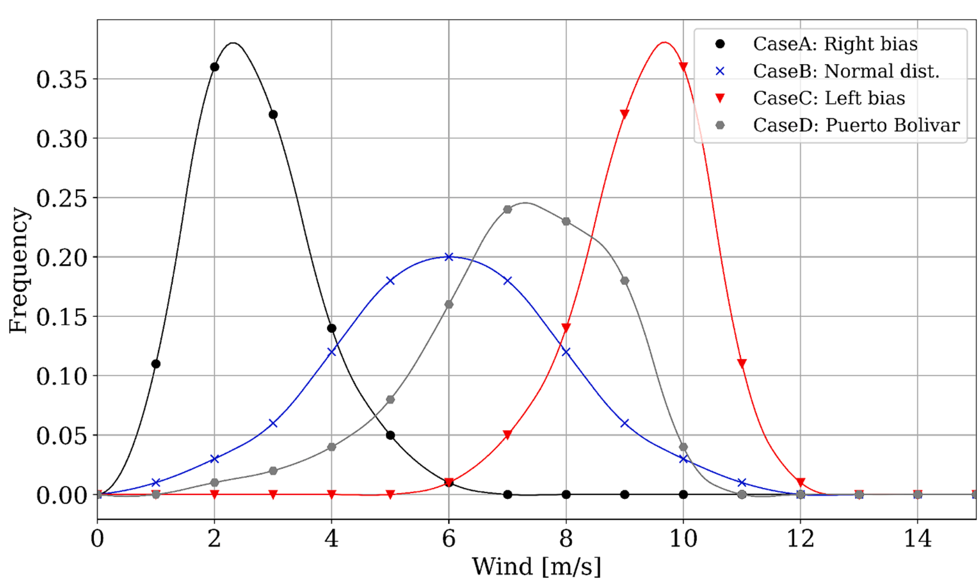

Fig. 2. Wind Speed probability distribution for study Cases.

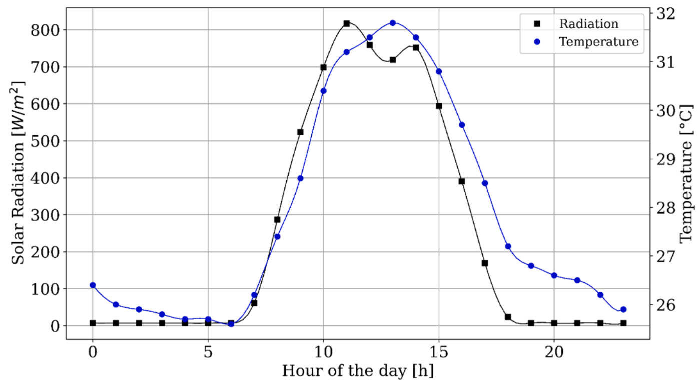

a)

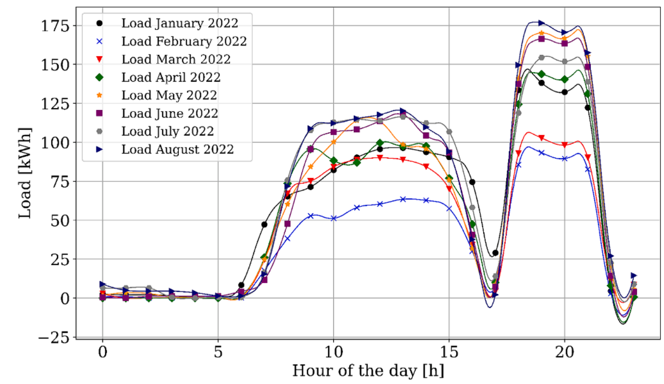

b)

Fig. 3. Daily profiles. a) Solar radiation and Temperature in Puerto Bolivar. b) Month load.

occurrence around 2 m/s. Consequently, the turbine is unlikely to reach its nominal electrical generation and will maintain a very high likelihood of at least starting the generation. On the other hand, the resource with a left bias statistical distribution exceeds the expectation of the cut-in speed. It has a higher probability of occurrence that is very close to the expected nominal speed of small wind turbines (around 12 m/s). It should be noted that high wind resources may not be available year-round, and lower resources may be more constant, as described by a typical probability distribution for wind resources such as the Weibull distribution [39].

All wind speed cases are integrated with typical solar radiation resources and temperature profiles from Puerto Bolivar, given for one day, as shown in Fig. 3a [38]. In this sense, the demand profile over the year is based on the data load from Uribia, La Guajira in 2022, which took values between 859 kWh/day (February 2022) and 1,630 kWh/day (August 2022) [40], following the daily profiles of Fig. 3b from January to August of 2022; for the months not reported, the demand profile is estimated by the highest values stated in August 2022.

3.1. HRES technological parameters

Regarding the technological parameters, for wind energy generation, this study considers a horizontal wind turbine with a nominal power P_r of 10.5 kW, cut-In Speed V_{ci} of 2 m/s, cut-Off Speed V_{co} equal to 30 m/s, and nominal speed V_r of 12 m/s [41]. The initial capital cost for the wind turbine $C_{c,wt}$ is set as 1,350 USD/kW, and its maintenance cost $C_{m,wt}$ of 4 % on $C_{c,wt}$ [42]. On the other hand, the nominal power of the photovoltaic panel P_{pvr} is 465 W with a temperature coefficient N_T of -0.0035 °C$^-$1, operating temperature $NOCT$ of 45 °C, and reference temperature T_{ref} of 25 °C [43]. The installation cost of a photovoltaic panel $C_{c,pv}$ is considered to be 0.2 USD/W; meanwhile, the maintenance cost $C_{m,pv}$ is estimated to be about 2 % of the total installation cost [42]. Additionally, the battery's nominal capacity S_b was 4.56 kWh, its efficiency η_{bat} took a value of 85 %, maximum discharge percentage DOD 95 %, self-discharge ratio σ of 0.002 %/h, its maximum charge and discharge rate r_{rb} 8 %, and the price of each battery 2,650 USD [44]. Finally, the capacity of the converter is 15 kW with an efficiency η_{inv} of 95 % and a price of 6,000 USD [25].

The above capacities for wind turbines, photovoltaic panels, batteries, and converters are selected based on commercial equipment on small and medium scales, considering the sizing scale that involves this study compared with the work developed by Torres et al. [25]. For the PSO sizing methodology, the number of particles p_{PSO} is 150, the characteristics of each particle n_{ch} took values between 0 and 1,500; for the velocity calculation, w_{pso} is set to 1.5, c_1 and c_2 are 2.5 and 3.5, respectively, and the number of iterations is 50.

Table 3
Values for Weight Sensitive Analysis.

Study	Technical factor weight (w_T)	Economic factor weight (w_E)	Environmental factor weight (w_{CO2})
WSA1	0.33	0.33	0.33
WSA2	0.25	0.50	0.25
WSA3	0.25	0.25	0.50

4. Results and discussion

This section presents the results obtained with the PSO methodology for Cases A to D, starting with the weight sensitivity analysis for the multi-objective function. Then, the results for Case D, following the same PSO optimisation methodology, are presented.

4.1. PSO weight value sensitivity analysis

To define the weighting values of each factor in Equation (11), this work presents a weighting sensitivity analysis (WSA) for the variations summarised in Table 3. The first variation of the sensitivity analysis (WSA1) considered that the technical, economic, and environmental factors have equal importance, obtaining a weighting of 33 % for each ($w_T = w_E = w_{CO2} = 0.33$). The following two variations considered that one of the factors (i.e., the economic or the environmental factor) had greater relevance in the sizing of the hybrid system. In contrast, the other two factors maintained equal importance. The technical factor was not considered as part of the sensitivity analysis since it is imposed as a constrain for the optimisation method, i.e., the solution tends to reach a value of 4 % of $LPSP$; however, a technical factor weight is imposed to ensure the participation of it in the optimisation process. The WSA2 study considered the economic factor to be of greater importance, so the economic weighting was set at 50 % ($w_E = 0.5$) and the weighting for the technical and environmental factors was 25 % ($w_T = w_{CO2} = 0.25$). The WSA3 variation considered the environmental evaluation as the most important factor with a 50 % weighting ($w_{CO2} = 0.5$), with the technical and economic factors both 25 % ($w_T = w_E = 0.25$).

The weighting studies of Table 3 are run ten times with the technical, economic, and environmental parametrisation described in section 3.1, considering the wind distributions from Fig. 2. Fig. 4 presents the comparation between the best solutions reached by the weighting study as function of $LCOE$ and ER_{CO_2}. The best solution for WSA1 correspond to the average of the solutions achieved with minimum $LPSP$, $LCOE$ and ER_{CO_2}, since the weights in this study were equal for the three factors of the multi-objective function. On the other hand, the values for WSA2 correspond to the best economic solution (minimum $LCOE$), while the values for WSA3 are those achieved with the best environmentally

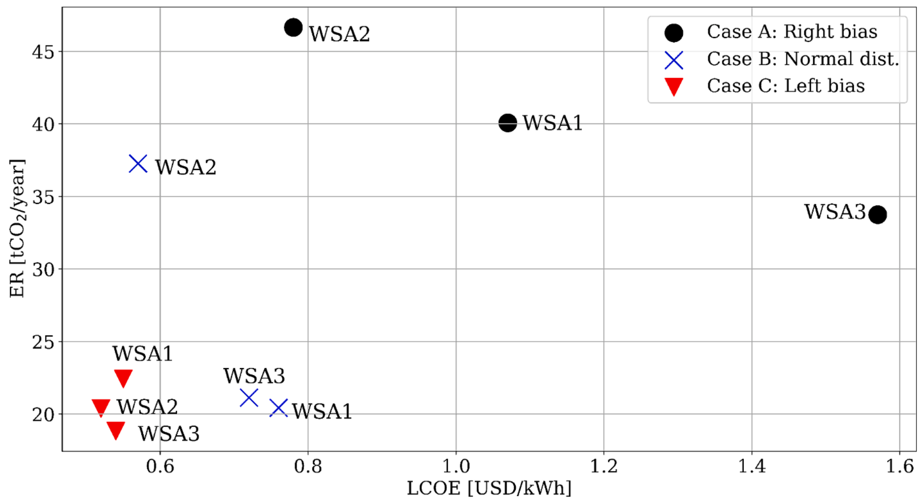

Fig. 4. Weighting Sensitive Analysis Results. Comparative results as a function of wind resource.

friendly configuration (minimum ER_{CO_2}).

Fig. 4 shows that the solutions for Case A (right-biased wind distribution) tended to be located to the right and at the top of the graph, obtaining higher values of levelized cost of energy and CO_2e emissions. This is due to the limited wind resources. Then, the sizing approach selects the solutions based on solar resources to generate electricity with higher pollutant rate emissions than wind energy (see Table 1). On the other hand, the solutions for Case C (left bias wind distribution) were in the lower-left corner of the mapping, i.e., presenting lower values for both the levelized energy cost and the pollutant emission rate. The above indicates that the sizing method gets a higher share of wind generation in the presence of an outstanding wind resource. Finally, the normal distribution in the wind resource used in Case B, allows to obtained solutions with similar values of ER_{CO_2}, and slightly higher *LCOE* than those for Case C, for the WSA1 and WSA3 weight studies. In this regard, a moderate wind resource is still used to size configurations with wind energy for cases where the environmental factor is relevant.

However, the configuration minimises costs when the economic factor becomes more critical (WSA2 solutions), as observed in Fig. 4. For Cases A and B, giving more importance to *LCOE*, the sizing model obtained configurations with much lower values of levelized cost than the solutions obtained by weighting cases WSA1 and WSA3 since it was preferred to integrate solar panels and batteries in the hybrid system, due to the limitations of the wind resource. However, in Case C, with an outstanding wind resource, the sizing tends to integrate wind turbines for all weighting cases, where the best configurations had similar values of *LCOE*. This solution is located to the left of the WSA1 and WSA3 solutions for all instances of wind resource variation. Moreover, if the wind resource is reduced (Cases A and B), the solution with the higher weight to the economic factor obtains higher pollution rates.

The share of wind generation is shown in Fig. 5, which compares the percentage value of each solution in Fig. 4. The obtained values of wind share for Case A were 18.5 %, 3.7 % and 36. 8 % for the weight cases WSA1, WSA2 and WSA3, respectively; all values were much lower than those obtained for Cases B and C; while the resource with the normal distribution obtained wind energy shares of 78.9 %, 29.4 % and 85.7 % for WSA1, WSA2 and WSA3, the resource with left bias distribution achieved 75.2 %, 78.9 % and 86.0 % for the factor weight cases. It is thus evident that the participation of wind turbine generation increases with the resource increase and when the environmental criterion is prioritized in the sizing.

Fig. 6 presents results for the studies when prioritising the economic and environmental factors (WSA2 and WSA3, respectively) to understand the sizing preference in selecting the renewable generation configuration. The participation of wind and solar generation over 24 h (1 day) of operation is observed, and the wind resource cases (Cases A to C) are also considered. In this way, the columns represent the variation of the weights of the factors, and the rows represent the variation in the wind resource to evaluate the participation in electricity generation. Observing the share of wind power generation, it is evident that as the wind resource increases, the electricity generation produced by small wind turbines increases too, regardless of the type of weight factor that prevails. The most interesting comparison comes from the analysis of each wind resource case (Case A, B or C) and the effect of changing the importance of the weighting factor. In all cases, there is a greater participation of wind generation when the environmental factor ER_{CO_2} is prioritized (Fig. 5b, 5d, and 5f).

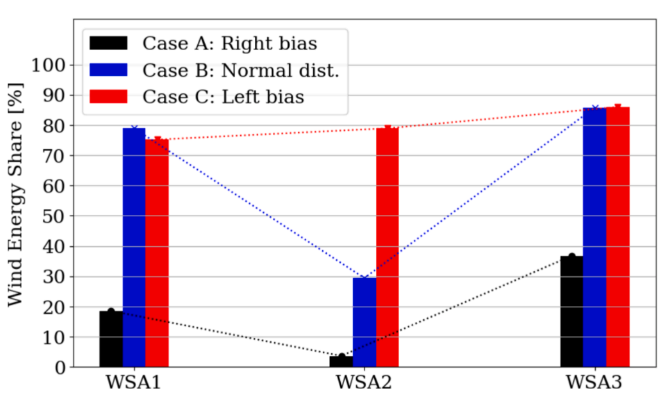

Fig. 5. Percentaje of wind energy share.

4.2. HRES sizing: Case D

The PSO optimisation was finally used for Case D of Puerto Bolivar, La Guajira (see Fig. 2). The sizing was performed considering the three cases of weighting analysis (WSA1 to WSA3), and for each case, the PSO optimisation algorithm was run ten times. The representative results of the weight analysis for Case D are mapped with the solutions obtained for Cases B and C, as given in Fig. 7, since the wind speed, according to the data extracted from the meteorological station, resembles the behaviour of a normal distributed resource, which tends slightly to a left bias, as shown Fig. 2.

The weighting analysis for case D shows that configurations with *LCOE* and ER_{CO_2} values similar to the normal (Case B) and left bias (Case C) wind resource distribution can be obtained. However, it is clear that by prioritizing the economic factor (WSA2), the configuration drasti-

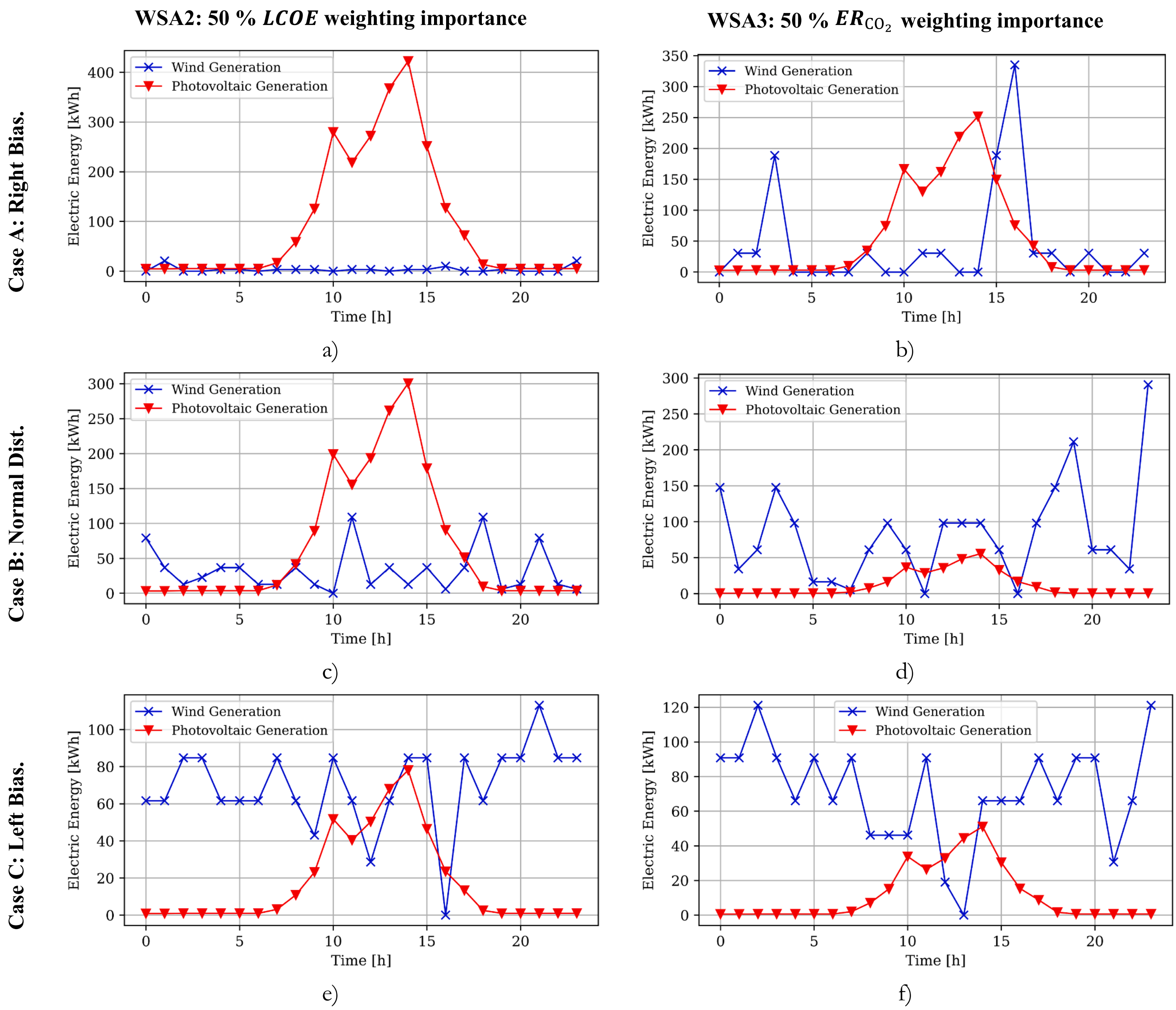

Fig. 6. Renewable electricity share is based on the weight of factors and wind resources. a) Case A and WSA2. b) Case A with WSA3. c) Case B with WSA2. d) Case B with WSA3. e) Case C with WSA2. f) Case C with WSA3.

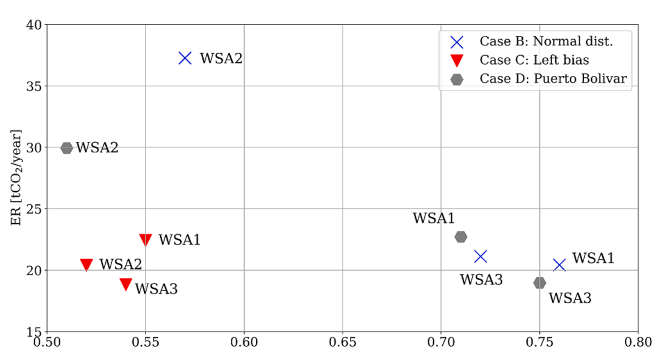

Fig. 7. Weighting analysis results of Case D, in contrast to results for Cases B and C.

cally reduces the levelized cost of energy, obtaining values close to those obtained for Case C, but with a higher emission rate. While by prioritizing the environmental factor (WSA3), configurations with similar *LCOE* and ER_{CO_2} values to those of Case B.

To evaluate the configuration of the hybrid renewable system when it is decided to prioritise the economic or environmental factor, the renewable electric generation share, the state of charge of the battery, and the total electricity generation of renewables are compared over two operations days in Fig. 8. The configuration obtained prioritising the economic factor (Case D with WSA2) reached *LCOE* value of 0.514 USD/kWh and emission rate ER_{CO_2} of 29.94 tCO_2e/year, corresponding to a configuration of 19 small wind turbines, 554 photovoltaic panels and 601 batteries, meaning a wind electricity generation of 49.1 %. On the other hand, the HRES configuration with environmental priority (Case D with WSA3) obtained a levelized cost of energy of 0.754 USD/kWh,an emission rate value of 18.97 tCO_2e/year and a wind energy share of 90.2 %, integrating 32 wind turbines, 98 photovoltaic panels and 832 batteries.

Comparing the renewable energy share (Fig. 8a and 8b), it is again evident that wind power is preferred over photovoltaic power when the priority is to reduce polluting emissions. The state of the batteries has a similar behaviour for two weight cases (Fig. 8c and 8d), varying significantly in the maximum storage capacity, being higher in the configuration with environmental priority, clearly coinciding with the number of batteries selected for the HRES sizing. The preference to use more batteries is also because the emission rate of batteries is lower than the solar panels based on the life cycle analysis; in this way, the sizing

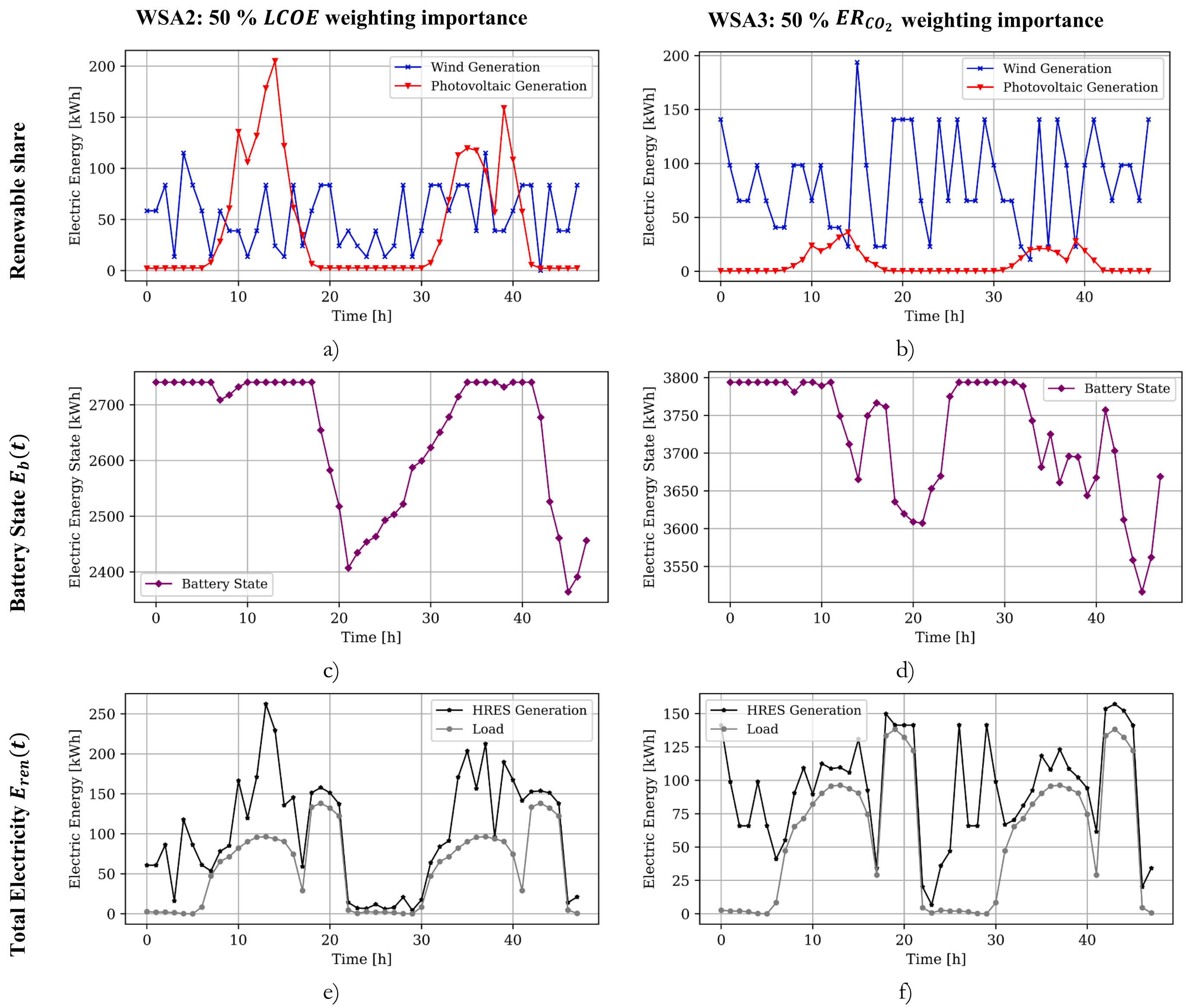

Fig. 8. Comparison of renewable energy share, battery charge status and total renewable generation. a) Renewable share Case D and WSA2. b) Renewable share Case D and WSA3. c) Battery state Case D and WSA2. d) Battery State Case D and WSA3. e) Total electricity generation Case D and WSA2. f) Total electricity generation Case D and WSA3.

directs the search for technologies with a lower environmental impact when the ER_{CO_2} factor is prioritised in the multi-objective function.

The preference to choose a higher share of wind and battery storage energy did not sacrifice the demand met, as shown by the comparison of the total electric energy generated by the HRES (Fig. 8e and 8f) since the generation adapts to the region's demand. This is consistent with the fact that the probability of load loss *LPSP* is a constraint factor in the search for the best configuration, which should be included in the multi-objective function to tend to minimise loss of power supply.

5. Conclusions

This study presented the sizing procedure for a hybrid renewable energy system (HRES) composed of wind energy, photovoltaic solar energy and battery bank storage. The design used the particle swarm optimization (PSO) algorithm with a multi-objective function, involving the technical factor of probability of loss of power supply (*LPSP*), the economic factor of levelized cost of energy (*LCOE*) and the environmental factor based on life cycle analysis and CO_2e emissions rate (ER_{CO_2}). The cases focused on the variation of the wind speed resource and the algorithm's response when finding a configuration of the HRES system. Case A presented a wind resource with a right bias (Low Resource), Case B was characterised by a resource with a normal frequency distribution (Intermediate Resource), Case C was characterised by a wind speed resource with a left bias (High Resource), and Case D represented the wind resource conditions of La Guajira in Colombia. For all cases, the solar resource and the ambient temperature were set according to the typical meteorological conditions of La Guajira.

For all study cases, the PSO optimisation found solutions with a technical performance that matched the loss of power supply probability restriction (*LPSP* maximum at 4 %). Moreover, the best economic and environmental configuration was obtained by evaluating Case C, where the best economic solution corresponds to the best environmental solution. As the wind resource improved, the share of wind energy in the hybrid system configuration increased. Furthermore, the most outstanding contribution of the weighting sensitivity analysis was to show the trend that if the priority of the environmental factor increases, the share of small wind turbines also increases. On the other hand, the case study for the Colombian context highlighted a resource with a behaviour similar to a normal distribution with a slight bias to the left. Here, the participation of wind generation was emphasised again. Still, the inclusion of a more significant number of batteries than in the solution obtained by prioritising the economic factor, agreeing that the sizing method directs the search to find technologies that satisfy energy demand with the lowest possible rate of polluting emissions.

It also can be inferred that the condition of obtaining the lowest *LCOE* values is closely related to increasing the emissions rate, which is associated with the low-cost option for electricity generation, which also has the highest specific emissions rate, such as with photovoltaic generation. Additionally, the magnitude of the wind resource is decisive to obtaining a reliable hybrid renewable energy system that is competitive in terms of the levelized cost of energy, and that also reduces CO_2e emission rates from the perspective of life cycle analysis, as demonstrated by the solution obtained for a wind resource with a left bias (i.e., high wind resource), where the solution has the lowest value of *LCOE* and also of ER_{CO_2}.

CRediT authorship contribution statement

José Luis Torres-Madroñero: Writing – original draft, Validation, Software, Investigation, Formal analysis. **César Nieto-Londoño:** Writing – review & editing, Supervision, Project administration, Funding acquisition, Formal analysis, Conceptualization. **Erika Arenas-Castiblanco:** Writing – review & editing, Supervision, Methodology, Formal analysis, Conceptualization. **Zulamita Zapata-Benabithe:** Writing – review & editing, Supervision, Formal analysis. **Hussam Jouhara:** Writing – review & editing, Supervision, Methodology, Conceptualization.

Declaration of competing interest

The authors declare that they have no known competing financial interests or personal relationships that could have appeared to influence the work reported in this paper.

Data availability

Data will be made available on request.

Acknowledgements

This work is part of research funded by the Universidad Pontificia Bolivariana through project 686C-08/21-19, “Study of the flexibility of generation and consumption systems for a sustainable energy transition”.

References

[1] A. K. Bansal, Sizing and forecasting techniques in photovoltaic-wind based hybrid renewable energy system: a review, Oct. 01, 2022, *Elsevier Ltd.* doi: 10.1016/j.jclepro.2022.133376.
[2] B.K. Das, M. Hasan, Optimal sizing of a stand-alone hybrid system for electric and thermal loads using excess energy and waste heat, Energy 214 (2021), https://doi.org/10.1016/j.energy.2020.119036.
[3] S. Saha, G. Saini, S. Mishra, A. Chauhan, S. Upadhyay, A comprehensive review of techno-socio-enviro-economic parameters, storage technologies, sizing methods and control management for integrated renewable energy system, Sustainable Energy Technol. Assess. 54 (2022), https://doi.org/10.1016/j.seta.2022.102849.
[4] A.G. Olabi, et al., Renewable energy systems: comparisons, challenges and barriers, sustainability indicators, and the contribution to UN sustainable development goals, Int. J. Thermofluids 20 (2023), https://doi.org/10.1016/j.ijft.2023.100498.
[5] A. Mahesh, G. Sushnigdha, Optimal sizing of photovoltaic/wind/battery hybrid renewable energy system including electric vehicles using improved search space reduction algorithm, J Energy Storage 56 (2022), https://doi.org/10.1016/j.est.2022.105866.
[6] D. Hill, et al., Techno-economic sensitivity analysis for combined design and operation of a small modular reactor hybrid energy system, Int. J. Thermofluids 16 (2022), https://doi.org/10.1016/j.ijft.2022.100191.
[7] A. Khanahmadi, R. Ghaffarpour, A cost-effective and emission-Aware hybrid system considering uncertainty: A case study in a remote area, Renew Energy 201 (2022) 977–992, https://doi.org/10.1016/j.renene.2022.10.031.
[8] D. Roy, R. Hassan, B.K. Das, A hybrid renewable-based solution to electricity and freshwater problems in the off-grid Sundarbans region of India: Optimum sizing and socio-enviro-economic evaluation, J Clean Prod 372 (2022), https://doi.org/10.1016/j.jclepro.2022.133761.
[9] A.G. Abo-Khalil, A. Sobhy, M.A. Abdelkareem, A.G. Olabi, Advancements and challenges in hybrid energy storage systems: components, control strategies, and future directions, Int. J. Thermofluids 20 (2023), https://doi.org/10.1016/j.ijft.2023.100477.
[10] J. Chang, et al., Multi-objective optimization of a novel combined cooling, dehumidification and power system using improved M-PSO algorithm, Energy 239 (Jan. 2022), https://doi.org/10.1016/j.energy.2021.122487.
[11] M. Thirunavukkarasu, Y. Sawle, H. Lala, A comprehensive review on optimization of hybrid renewable energy systems using various optimization techniques, Apr. 01, 2023, *Elsevier Ltd.* doi: 10.1016/j.rser.2023.113192.
[12] P. Singh, M. Pandit, L. Srivastava, Multi-objective optimal sizing of hybrid micro-grid system using an integrated intelligent technique, Energy 269 (2023), https://doi.org/10.1016/j.energy.2023.126756.
[13] J. Lian, Y. Zhang, C. Ma, Y. Yang, and E. Chaima, A review on recent sizing methodologies of hybrid renewable energy systems, Nov. 01, 2019, *Elsevier Ltd.* doi: 10.1016/j.enconman.2019.112027.
[14] F.S. Mahmoud, et al., Optimal sizing of smart hybrid renewable energy system using different optimization algorithms, Energy Rep. 8 (2022) 4935–4956, https://doi.org/10.1016/j.egyr.2022.03.197.
[15] P. Rullo, L. Braccia, P. Luppi, D. Zumoffen, D. Feroldi, Integration of sizing and energy management based on economic predictive control for standalone hybrid renewable energy systems, Renew Energy 140 (2019) 436–451, https://doi.org/10.1016/j.renene.2019.03.074.
[16] R. Hassan, B.K. Das, M. Hasan, Integrated off-grid hybrid renewable energy system optimization based on economic, environmental, and social indicators for sustainable development, Energy 250 (2022), https://doi.org/10.1016/j.energy.2022.123823.
[17] M. Maleki Tehrani, M. Akhtari, A. Kasaeian, M. A. Vaziri Rad, A. Toopshekan, and M. Sadeghi Motlagh, Techno-economic investigation of a hybrid biomass renewable energy system to achieve the goals of SDG-17 in deprived areas of Iran, *Energy Convers. Manag.*, 291, 2023, 10.1016/j.enconman.2023.117319.
[18] H. Yazdani, M. Baneshi, M. Yaghoubi, Techno-economic and environmental design of hybrid energy systems using multi-objective optimization and multi-criteria decision making methods, Energy Convers. Manag. 282 (2023), https://doi.org/10.1016/j.enconman.2023.116873.
[19] A. Toopshekan, P. Rahdan, M.A. Vaziri Rad, H. Yousefi, F.R. Astaraei, Evaluation of a stand-alone CHP-Hybrid system using a multi-criteria decision making due to the sustainable development goals, Sustain Cities Soc. 87 (2022) Dec, https://doi.org/10.1016/j.scs.2022.104170.
[20] J. Więckowski and W. Sałabun, Sensitivity analysis approaches in multi-criteria decision analysis: a systematic review, Nov. 01, 2023, *Elsevier Ltd.* doi: 10.1016/j.asoc.2023.110915.
[21] S.R. Tito, T.T. Lie, T.N. Anderson, Optimal sizing of a wind-photovoltaic-battery hybrid renewable energy system considering socio-demographic factors, Sol. Energy 136 (2016) 525–532, https://doi.org/10.1016/j.solener.2016.07.036.
[22] A. Maleki, F. Pourfayaz, Optimal sizing of autonomous hybrid photovoltaic / wind / battery power system with LPSP technology by using evolutionary algorithms, Sol. Energy 115 (2015) 471–483, https://doi.org/10.1016/j.solener.2015.03.004.
[23] C.A. Marenco-Porto, J.L. Torres-Madroñero, C. Nieto-Londoño, E. Arenas-Castiblanco, Z. Zapata-Benabithe, H. Vidal-Gutiérrez, Hybrid renewable energy systems sizing for the Colombian context by multiple attribute decision making evaluation, AIP Conference Proceed. 2872 (1) (2023) 020007, https://doi.org/10.1063/5.0163247.
[24] A. Malheiro, P.M. Castro, R.M. Lima, A. Estanqueiro, Integrated sizing and scheduling of wind/PV/diesel/battery isolated systems, Renew Energy 83 (2015) 646–657, https://doi.org/10.1016/j.renene.2015.04.066.
[25] J.L. Torres-Madroñero, C. Nieto-Londoño, J. Sierra-Pérez, Hybrid energy systems sizing for the colombian context: A genetic algorithm and particle swarm optimization approach, Energies (basel) 13 (21) (2020) Nov, https://doi.org/10.3390/en13215648.
[26] HOMER Energy, “COE – HOMER PRO.” [Online]. Available: https://www.homerenergy.com/products/pro/docs/latest/levelized_cost_of_energy.html.
[27] S. Mandal, B.K. Das, N. Hoque, Optimum sizing of a stand-alone hybrid energy system for rural electrification in Bangladesh, J Clean Prod 200 (Nov. 2018) 12–27, https://doi.org/10.1016/j.jclepro.2018.07.257.
[28] A.-R. Ali, N. Bartie, J. Husmann, F. Cerdas, D. Schröder, C. Herrmann, Simulation-based life cycle assessment of secondary materials from recycling of lithium-ion batteries, Resour. Conserv. Recycl. 202 (2024) 107384, https://doi.org/10.1016/j.resconrec.2023.107384.
[29] B. Shi, W. Wu, L. Yan, Size optimization of stand-alone PV/wind/diesel hybrid power generation systems, J. Taiwan Inst. Chem. Eng. 73 (2017) 93–101, https://doi.org/10.1016/j.jtice.2016.07.047.
[30] S. Nicholson, G. Heath, “Life Cycle Greenhouse Gas Emissions from Electricity Generation: Update Life Cycle Assessment of Energy Systems,” 2021. [Online]. Available: https://data.nrel.gov/submissions/171.
[31] E. Ates, N. Karaarslan, Investigation of hybrid renewable energy green house for reducing residential carbon emissions, Int. J. Thermofluids 21 (2024) 100558, https://doi.org/10.1016/j.ijft.2023.100558.

[32] NREL and National Renewable Energy Laboratory, "Life Cycle Greenhouse Gas Emissions PV," 2012.
[33] NREL and National Renewable Energy Laboratory, "Life Cycle Greenhouse Gas Emissions WT," 2012.
[34] H. Borhanazad, S. Mekhilef, V. Gounder Ganapathy, M. Modiri-Delshad, A. Mirtaheri, Optimization of micro-grid system using MOPSO, Renew Energy 71 (2014) 295–306, https://doi.org/10.1016/j.renene.2014.05.006.
[35] CREG and Comisión de Regulación de Energía y Gas, "RESOLUCIÓN No.082.".
[36] U.S. Energy Information Administration, "Levelized Costs of New Generation Resources in the Annual Energy Outlook 2022," 2022.
[37] A. Maleki, A. Askarzadeh, Comparative study of artificial intelligence techniques for sizing of a hydrogen-based stand-alone photovoltaic / wind hybrid system, Int. J. Hydrogen Energy 9 (2014).
[38] IDEAM, "Instituto de Hidrología, Meteorología y Estudios Ambientales," 2019.
[39] J. L. Torres-Madroñero, J. Alvarez-Montoya, D. Restrepo-Montoya, J. M. Tamayo-Avendaño, C. Nieto-Londoño, J. Sierra-Pérez, Technological and Operational Aspects That Limit Small Wind Turbines Performance, pp. 1–39, 2020, doi: 10.3390/en13226123.
[40] I. Instituto de Planificación y Promoción de Soluciones Energéticas, "Informe Mensuales Telemetría." Accessed: Jul. 23, 2023. [Online]. Available: https://ipse.gov.co/cnm/informe-mensuales-telemetria/.
[41] ENAIR, "Wind Turbine ENAIR 160." Accessed: Jul. 23, 2023. [Online]. Available: https://www.enair.es/en/.
[42] I. Renewable Energy Agency, *Renewable power generation costs in 2021*. 2022. [Online]. Available: www.irena.org.
[43] JA SOLAR, "465W Half-Cell Module." Accessed: Jul. 23, 2023. [Online]. Available: https://www.jasolar.com/html/en/.
[44] Bornay, "PYLONTECH." Accessed: Jul. 23, 2023. [Online]. Available: https://www.bornay.com/en.